Galla Rhois water extract inhibits lung metastasis by inducing AMPK-mediated apoptosis and suppressing metastatic properties of colorectal cancer cells

JEONG-GEON MUN[1*], JI-YE KEE[1*], YO-HAN HAN[1], SULLIM LEE[2], SEONG-HWAN PARK[1], HEE DONG JEON[1] and SEUNG-HEON HONG[1]

[1]Department of Oriental Pharmacy, College of Pharmacy, Wonkwang-Oriental Medicines Research Institute, Wonkwang University, Iksan, Jeonbuk 54538; [2]Department of Life Sciences, College of Bio-Nano Technology, Gachon University, Seongnam 13120, Republic of Korea

Received March 29, 2018; Accepted October 9, 2018

DOI: 10.3892/or.2018.6812

Abstract. Galla Rhois is a commonly used medicine in East Asia for the treatment of several diseases. However, the effects of Galla Rhois on the metastasis of colorectal cancer (CRC) and the underlying molecular mechanisms have not been studied. We investigated the anti-metastatic properties of Galla Rhois water extract (GRWE) on metastatic CRC cells. The effect of GRWE on the viability of colon 26 (CT26) cells was evaluated using WST-8 assay. Annexin V assay and western blot analysis were performed to elucidate the underlying molecular mechanisms involved in apoptosis. GRWE suppressed viability of CT26 cells by inducing apoptosis through the cleavage of caspase-3 and PARP, downregulation of caspase-8, caspase-9, Bcl-2 and Bcl-xL, and upregulation of Bax. Metastatic phenotypes such as epithelial-mesenchymal transition (EMT), migration, and invasion of CRC cells were investigated by real-time reverse transcription polymerase chain reaction, wound healing assay, and matrigel invasion assay, respectively. Non-cytotoxic concentrations of GRWE inhibited EMT in CRC cells by regulating the expression of EMT markers. GRWE attenuated cell migration and invasion through the inhibition of matrix metalloproteinase (MMP)-2 and MMP-9 activity. Moreover, GRWE suppressed colorectal lung metastasis *in vivo*, suggestive of its potential application for the treatment of colorectal metastasis.

Correspondence to: Professor Seung-Heon Hong, Department of Oriental Pharmacy, College of Pharmacy, Wonkwang-Oriental Medicines Research Institute, Wonkwang University, 460 Iksandae-ro, Iksan, Jeonbuk 54538, Republic of Korea
E-mail: jooklim@wku.ac.kr

*Contributed equally

Key words: Galla Rhois, colorectal metastasis, apoptosis, AMPK, EMT

Introduction

Colorectal cancer (CRC) is one of the most common cancers and the leading cause of cancer-related deaths throughout the world (1). Approximately 1.4 million new cases are identified each year and almost 694,000 deaths are reported (2). Metastasis from CRC develops in 40-60% of patients and the most frequent sites of metastasis for CRC are the liver and lungs (3). The 5-year survival rate with surgical resection of liver and lung metastasis is 30-40 and 31-48%, respectively. However, candidates for surgical resection of liver and lung metastatic disease include 10-25% and less than 10% of patients, respectively (4,5). Of these cases, metastatic CRC is a crucial cause of morbidity and mortality (6).

Metastasis is a complex series of steps that involves the spread of tumor cells or pathogens from the primary lesion to distant parts of the body. It is simply divided into the processes of invasion, intravasation, and extravasation. Tumor cells that lose the cell-cell adhesion capacity and gain cellular motility invade the surrounding stroma via degradation of the basement membrane and extracellular matrix (ECM). The detached cells enter the lymph nodes and blood vessels and circulate to remote sites. Once the circulating cells have arrived at the targeted organs, they adhere to, and penetrate into, the endothelium and basement membrane, followed by initiation of angiogenesis and proliferation (7). Metastatic cancer may be treated with chemotherapy, hormone therapy, immunotherapy, radiation therapy, resection, and combination of these methods (8). However, it may be difficult to treat once the cancer has spread, resulting in poorer prognosis.

Activation of epithelial-mesenchymal transition (EMT) plays an important role in the initial step of the metastatic cascade by increasing cell migration and invasion. EMT is a process by which epithelial cells undergo functional and biochemical changes to acquire mesenchymal cell phenotypes (9). The acquisition of mesenchymal phenotypes leads to the loss of cell polarity and adherent tight junction, resulting in the increase of motility and invasiveness. The characteristic features of EMT are downregulation of

epithelial markers and adherent tight junction proteins such as E-cadherin, desmosomes, and cytokeratins as well as upregulation of mesenchymal markers, including N-cadherin and vimentin (10). EMT is correlated with several cancer types, including prostate, ovarian, breast and CRC (11).

Apoptosis is a form of programmed cell death characterized by cellular changes, including cell shrinkage, chromatin condensation, and nuclear fragmentation while avoiding inflammation (12). Caspases are a family of proteolytic enzymes that regulate cell death and their activity is essential for the induction of apoptosis. Apoptotic caspases are divided into initiator and executioner caspases. Initiator caspases such as caspase-8 and caspase-9 activate several executioner caspases, resulting in the induction of apoptotic morphological changes (13). Poly ADP-ribose polymerase (PARP) is a nuclear enzyme related to several processes, including DNA repair, DNA stability and cell death (14). The anti-apoptotic factor Bcl-2 family proteins suppress apoptosis by preventing the release of the apoptosis-inducing factor from the mitochondria. Conversely, Bax is a pro-apoptotic protein that may trigger the activation of caspases, resulting in cell death (15). Apoptosis reduction or resistance is important for carcinogenesis and malignant transformation of cancer (16). Therefore, many cancer treatment strategies have been designed to induce apoptosis through the regulation of apoptotic signaling pathways.

Adenosine monophosphate-activated protein kinase (AMPK) is a major regulator that maintains energy homeostasis and cell proliferation. Activation of AMPK can promote energy production and conservation processes such as glycolysis and autophagy and inhibit energy consuming reactions including lipid synthesis (17-19). Particularly, AMPK can suppress carcinogenesis by inducing apoptosis and autophagy in CRC cells (20). AMPK activation is also associated with reduction of cancer mortality and good prognosis in CRC (21).

Galla Rhois is an insect gall produced by the Chinese sumac aphid (*Melaphis chinensis* Bell) on *Rhus chinensis* (22). In traditional Korean medicine, Galla Rhois constrains the lungs to suppress cough and excessive perspiration, astringes the intestine to check diarrhea, secures essence, and stops bleeding (23). In addition, Galla Rhois displays various pharmacological activities, including antioxidant, antidiabetic, anti-inflammatory, anti-anaphylactic, antibacterial, antiviral, and antidiarrheal effects (24,25). Galla Rhois contains several components such as methyl gallate, gallic acid, 1,2,3,4,6-penta-O-galloyl-β-d-glucose (PGG), and gallotannin (GT). Previous studies have reported that these compounds exhibit antitumor and anti-metastatic effects in breast cancer and fibrosarcoma (26-28). We hypothesize that Galla Rhois water extract (GRWE) may inhibit the metastatic ability of CRC cells. The anti-metastatic effect and related molecular mechanism of Galla Rhois in CRC are unclear. In the present study, we investigated the anti-metastatic properties and underlying mechanism of GRWE using metastatic CRC cell lines and an experimental metastatic model.

Materials and methods

Preparation of GRWE. Galla Rhois was purchased from Omniherb (Uiseong, Korea), which is a good manufacturing practices (GMP) certified company by the Korea Food and Drug Administration. To prepare GRWE, Galla Rhois (100 g) was boiled at 100˚C for 3 h with 1 l of distilled water (DW). The extract was filtered through Whatman filter paper and lyophilized. The samples were used for the treatment of cells after dissolving in DW and filtering using a 0.22-μm syringe filter. The yield of the dried extract from the starting materials was about 12.03%.

Cell culture. The murine colorectal carcinoma cell line colon 26 (CT26) and human colorectal adenocarcinoma cell line (HT29) were obtained from Korean Cell Line Bank (Seoul, Korea). Cells were cultured in Dulbecco's modified Eagle's medium (DMEM) containing 10% heat-inactivated fetal bovine serum (FBS) and 1% penicillin-streptomycin (all from Gibco-BRL; Thermo Fisher Scientific, Inc., Waltham, MA, USA) at 37˚C in an atmosphere of 5% CO_2.

Animals. The *in vivo* experiment was approved and performed in accordance with the internationally accepted principles for the care and use of laboratory animals by the Institutional Animal Care and Use Committee of Wonkwang University (WKU16-11). Twenty-four female BALB/c mice (4 weeks old, 17-18 g) were purchased from Samtako (Osan, Korea). The mice with *ad libitum* access to food and water were housed (8 mice/cage) in a laminar air-flow room with a controlled 12-h light/dark cycle at a constant temperature of 23±1˚C and humidity of 55±1%.

Assays of cell viability. Water-soluble tetrazolium salt-8 reagent (WST-8; Enzo Life Sciences, Farmingdale, NY, USA) was used for quantifying cell viability. CT26 cells ($2x10^3$ cells/well) and HT29 cells ($1x10^4$ cells/well) were seeded in 96-well plates and cultured overnight. The cells were treated with GRWE (20-100 μg/ml). After 24, 48 and 72 h of incubation, WST-8 reagent was mixed with new medium and added to each well. The absorbance was measured by microplate reader at 450 nm wavelength.

Apoptosis analysis. After GRWE (10-100 μg/ml) treatment for 24 h, the cells were collected and suspended in serum-containing medium. Cells ($1x10^5$ cells/100 μl) were transferred to a new tube and mixed with Muse™ Annexin V & Dead Cell Reagent (EMD Millipore, Billerica, MA, USA). Samples were incubated for 20 min in the dark and the apoptotic cells were measured by Muse™ Cell Analyzer (EMD Millipore).

Antibodies. Anti-PARP (cat. no. 9532), caspase-3 (cat. no. 14220), cleaved caspase-3 (cat. no. 9664), caspase-8 (cat. no. 4790), caspase-9 (cat. no. 9508), Bcl-xL (cat. no. 2764), phospho-AMPK (cat. no. 2535), AMPK (cat. no. 2532), phospho-extracellular signal-regulated kinase (ERK) (cat. no. 4370), phospho-p38 (cat. no. 4511), E-cadherin (cat. no. 3195) and N-cadherin (cat. no. 13116) antibodies were purchased from Cell Signaling Technology, Inc. (Danvers, MA, USA). Bcl-2 (cat. no. sc-7382), Bax (cat. no. sc-7480), ERK (cat. no. sc-94), p38 (cat. no. sc-7149), vimentin (cat. no. sc-6260), twist (cat. no. sc-81417), and glyceraldehyde 3-phosphate dehydrogenase (GAPDH) (cat. no. sc-47724) antibodies were purchased from Santa Cruz Biotechnology, Inc.

(Santa Cruz, CA, USA). Anti-rabbit (cat. no. 111-035-003) and anti-mouse (cat. no. 115-035-062) secondary antibodies were purchased from Jackson ImmunoResearch Laboratories, Inc. (Pennsylvania, PA, USA). All antibodies were diluted 1:1,000 in 3% skim milk (BD Biosciences, San Diego, CA, USA).

Western blot analysis. CT26 cells ($3x10^5$ cells/well) were seeded in a 6-well plate and treated with GRWE (10, 50 and 100 μg/ml). After treatment for 24 h, the cells were lysed with ice-cold lysis buffer (iNtRON Biotech, Seoul, Korea) for 1 h. Total lysates were centrifuged at 14,000 x g for 10 min, and the supernatants were collected for the determination of the extracted protein concentration using the Lowry method. Samples were mixed with 2X buffer, separated by sodium dodecyl sulfate polyacrylamide gel electrophoresis (SDS-PAGE) using 10% acrylamide gels and transferred onto polyvinylidene fluoride (PVDF) membranes. The membranes were incubated with 5% skim milk for at least 1 h. After washing with 0.1% PBST (0.1% Tween-20 in PBS), the membranes were incubated with primary antibodies for 3 h, followed by their treatment with horseradish peroxidase-conjugated secondary antibodies for 1 h at room temperature. The protein blots were detected using an enhanced chemiluminescence (ECL) system (Santa Cruz Biotechnology, Inc.). The density of western blot bands was quantified by densitometric analysis using ImageJ software (National Institutes of Health, Bethesda, MD, USA).

Real-time reverse transcription polymerase chain reaction (RT-PCR). RNA-spin™ extraction Kit (iNtRON Biotech) was used to extract total RNA in accordance with the manufacturer's protocol. First-strand cDNA synthesis was performed using High Capacity RNA-to-cDNA Kit (Applied Biosystems; Thermo Fisher Scientific, Inc.). Reverse transcription was conducted at 37˚C for 60 min and then at 95˚C for 5 min. Real-time RT-PCR was carried out using a Power SYBR® Green PCR Master Mix with a StepOnePlus™ Real-Time PCR System (Applied Biosystems; Thermo Fisher Scientific, Inc.). The PCR cycling condition was as follows: one cycle at 95˚C for 10 min, then 40 cycles of 95˚C for 15 sec, 60˚C for 1 min, 95˚C for 15 sec and melt curve at 60˚C for 1 min, 95˚C for 15 sec. Sequences of the primers used for murine genes were as follows: E-cadherin, 5'-AATGGCGGCAATGCAATCCCAAGA-3' and 5'-TGCCACAGACCGATTGTGGAGATA-3'; N-cadherin, 5'-TGGAGAACCCCATTGACATT-3' and 5'-TGATCCCTCAGGAACTGTCC-3'; vimentin, 5'-CGGAAAGTGGAATCCTTGCA-3' and 5'-CACATCGATCTGGACATGCTG-3'; Twist, 5'-AGCTACGCCTTCTCCGTCT-3' and 5'-TCCTTCTCTGGAAACAATGACA-3'; MMP-2, 5'-CCCCATGAAGCCTTGTTTACC-3' and 5'-TTGTAGGAGGTGCCCTGGAA-3'; MMP-9, 5'-AGACCAAGGGTACAGCCTGTTC-3' and 5'-GGCACGCTGGAATGATCTAAG-3'; GAPDH, 5'-GACATGCCGCCTGGAGAAAC-3' and 5'-AGCCCAGGATGCCCTTTAGT-3'. The mRNA expression of genes was normalized to the expression of the gene encoding GAPDH. The real-time RT-PCR data was analyzed using comparative Cq method (29).

Immunofluorescence. CT26 cells ($3x10^3$ cells/well) were grown on an 8-well chamber slide (Thermo Fisher Scientific, Inc.) and treated with GRWE. The cells were fixed in 4% paraformaldehyde for 15 min and permeabilized with 0.1% Triton X-100 for 10 min. After blocking with blocking buffer (3% bovine serum albumin and 0.3% Triton X-100 in PBS), the cells were incubated with the primary antibody at 4˚C, overnight. Following incubation, the cells were treated with Alexa Fluor 488-conjugated secondary antibody (Thermo Fisher Scientific, Inc.) for 2 h and nuclei stained with 4',6-diamidino-2-phenylindole (DAPI) (Sigma-Aldrich; Merck KGaA, Darmstadt, Germany). Images were acquired using a fluorescence microscope (Zeiss Observer A1 microscope; Carl Zeiss AG, Oberkochen, Germany).

Wound healing assay. CT26 cells ($5x10^5$ cells/well) were grown in a 6-well plate to form a confluent monolayer. A wound was created using a 200-μl micropipette tip and the detached cells were removed. The cells were treated with GRWE (1, 5 and 10 μg/ml) in the absence of FBS for 48 h. Images were captured under EVOS® XL Core Imaging System (Thermo Fisher Scientific, Inc.).

Invasion assay. Matrigel-coated BD Falcon cell culture chamber (BD Biosciences) was used to estimate the invasive activity of cancer cells. The lower wells were filled with 750 μl DMEM containing 10% FBS. Cells ($5x10^4$ cells) were seeded in the upper part of the transwell chambers in 200 μl FBS-free DMEM with GRWE (1, 5 and 10 μg/ml) and chambers were placed on a 24-well plate for 24 h. The upper inserts were fixed with 3.7% formaldehyde in PBS and washed twice with PBS. The fixed cells were permeabilized with methanol for 25 min and stained with Giemsa solution (Sigma-Aldrich; Merck KGaA) for 25 min. The inner sides of the chambers were cleaned with a swab and dried. The stained cells were observed under EVOS® XL Core Imaging System.

Zymography. For gelatin zymography, CT26 cells ($5x10^5$ cells/well) were seeded in a 6-well plate and treated with GRWE for 24 h. The supernatant from the GRWE-treated cells was mixed with 2X zymogram sample buffer (KOMA Biotech, Seoul, Korea) and the samples were electrophorized using SDS polyacrylamide gel containing 1% gelatin in the zymogram running buffer (KOMA Biotech). The gel was renatured in zymogram renaturing buffer for 30 min and incubated in zymogram developing buffer (both from KOMA Biotech) at 37˚C overnight. The gel was stained with Brilliant Blue R staining solution (ELPIS Biotech, Daejeon, Korea) for 30 min.

Experimental lung metastatic mouse model. CT26 cells ($1x10^5$ cells/200 μl PBS/mouse) were injected into mice via the lateral tail vein. GRWE and DW were orally administrated 2 h prior to the injection of CT26 cells and then, every day. The mice were sacrificed by cervical dislocation after 14 days and lung tissues were stained and fixed with Bouin's solution (Sigma-Aldrich; Merck KGaA). The weight of the lungs was measured and the number of nodules in the lungs was counted to evaluate CRC metastasis.

High-performance liquid chromatography (HPLC) analysis. During analysis of GT from GRWE, GT (molecular weight: 1701.20 g/mol; molecular formula: $C_{76}H_{52}O_{46}$; Santa Cruz Biotechnology, Inc.) was used as the standard. GRWE and

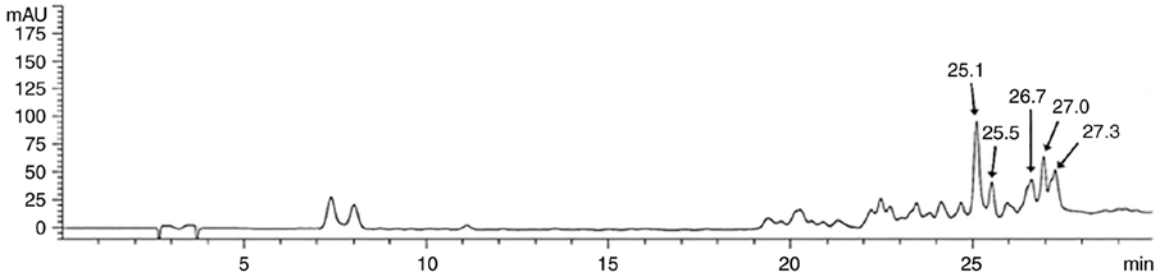

Figure 1. HPLC chromatograms of GRWE. GRWE, Galla Rhois water extract.

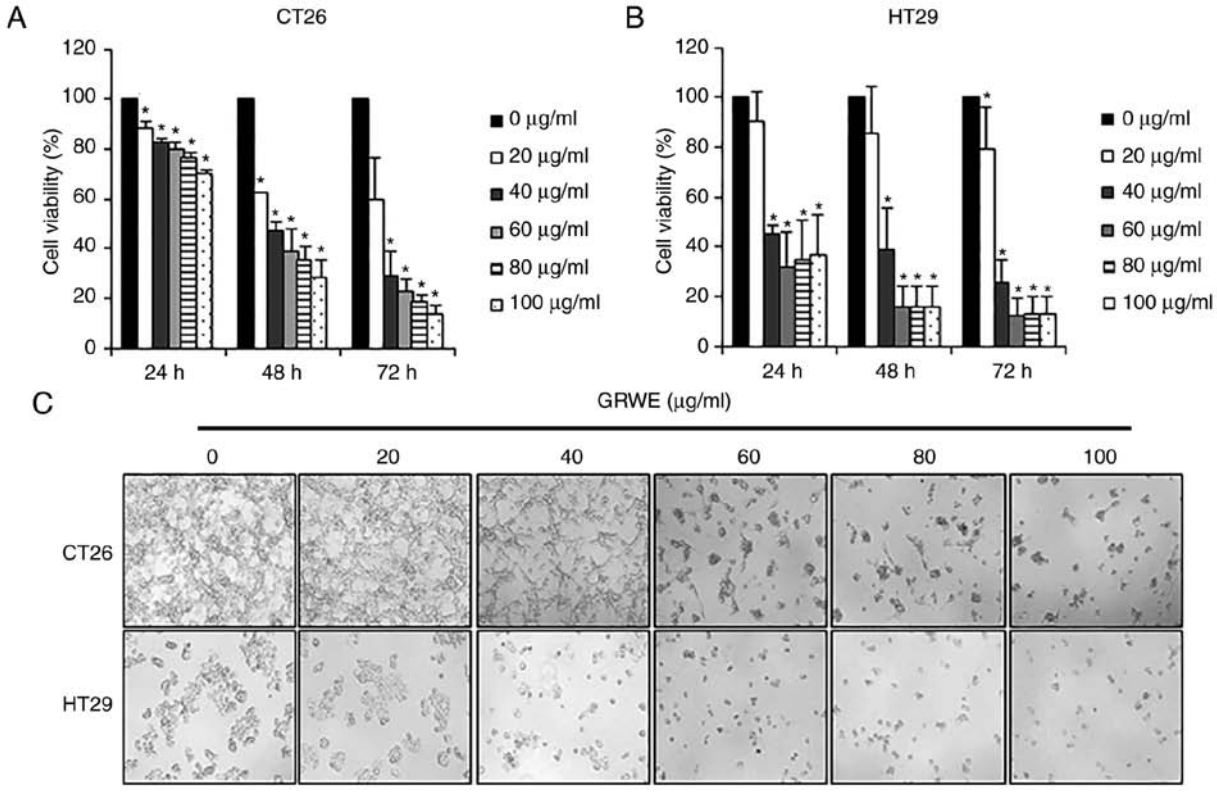

Figure 2. GRWE decreases cell viability in metastatic CRC cells. (A and B) Cell viability of GRWE-treated (A) CT26 and (B) HT29 cells. The cells were treated with GRWE at final concentrations of 20-100 μg/ml. Cell viability was determined using WST-8 reagent after 24, 48 and 72 h of treatment. (C) Morphology of GRWE-treated CT26 and HT29 cells. Images were captured by a microscope after 72 h of incubation with GRWE. Results are expressed as the mean ± SD of three independent experiments. *P<0.05. GRWE, Galla Rhois water extract.

the standard compound were dissolved in methanol (MeOH) and filtered through a 0.45-μm syringe filter before injection. An HPLC system comprised of an Agilent 1200 Series HPLC system (Agilent Technologies, Santa Clara, CA, USA) with a UV-vis detector was used. Separation was carried out on an YMC-Triart C_{18} column (150x4.6 mm I.D., 5 μm,) maintained at 40˚C. The mobile phase was comprised of solvent A (0.1% formic acid in water) and solvent B (0.1% formic acid in acetonitrile). The gradient condition of the mobile phase was as follows: 0-5 min, 15% A; 5-10 min, 15-20% A; 10-25 min, 20-35% A; 25-30 min, 35-15% A. Analysis was performed at a flow rate of 1.0 ml/min with the detection wavelength fixed at 280 nm (Fig. 1).

Statistical analysis. All data were presented as the mean ± standard deviation (SD). ANOVA with Tukey's post hoc test was used to determine the statistical significance. SPSS Statistics v18 (IBM Corp., Armonk, NY, USA) was used as the statistical analysis software. A value of P<0.05 was considered to indicate a statistically significant difference.

Results

Effect of GRWE on the proliferation of CRC cells. To investigate the cytotoxicity of GRWE on metastatic CRC cells, cell viability was determined by WST-8 assay. CT26 and HT29 cells were treated with GRWE at concentrations of 20-100 μg/ml. As shown in Fig. 2A and B, the viability of GRWE-treated cells decreased as compared with that of the control cells. Furthermore, treatment with GRWE for 72 h resulted in morphological changes in CT26 and HT29 cells (Fig. 2C).

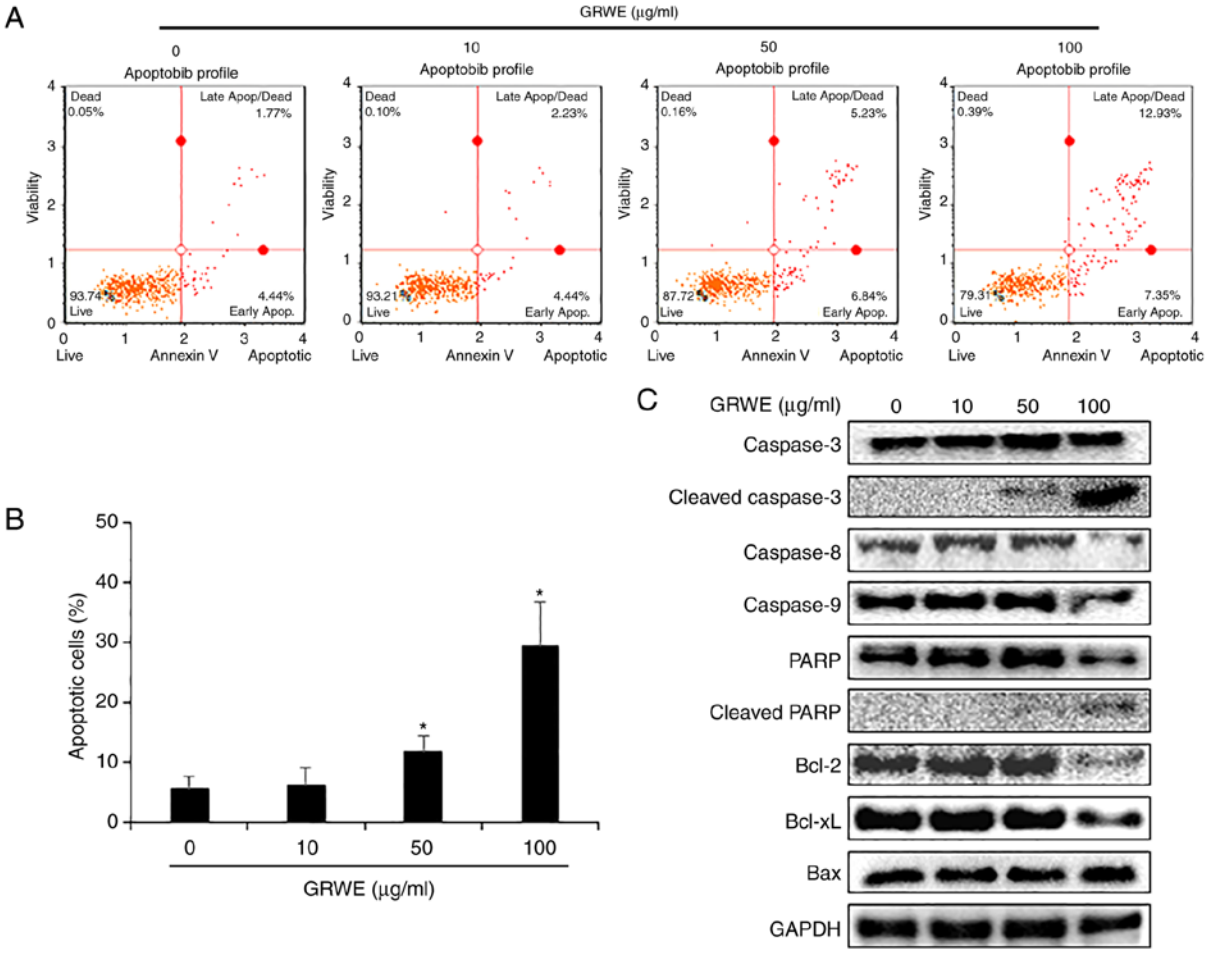

Figure 3. GRWE induces apoptosis in CT26 cells through extrinsic and intrinsic pathways. (A) CT26 cells were incubated with GRWE (10, 50, and 100 μg/ml) for 24 h and stained with Annexin V and 7-AAD. The image is a representative of three independent experiments. (B) The statistical graph of apoptotic cells from Annexin V staining at different concentrations of GRWE is displayed. (C) CT26 cells were treated with the indicated concentrations of GRWE for 24 h. The expression of caspase-3, cleaved caspase-3, caspase-8, caspase-9, PARP, cleaved PARP, Bcl-2, Bcl-xL and Bax were detected by western blotting using corresponding antibodies. Results are expressed as the mean ± SD of three independent experiments. *P<0.05. GRWE, Galla Rhois water extract.

Apoptotic effect of GRWE on CT26 cells. Annexin V assay was performed after treatment of cells with GRWE (10, 50, and 100 μg/ml) for 24 h to determine whether GRWE-induced cell death was related to the apoptosis of cells. As shown in Fig. 3A and B, treatment with GRWE resulted in an increase in the apoptosis of CT26 cells in a dose-dependent manner. To further investigate the mechanisms underlying GRWE-induced apoptosis, the expression of apoptosis-related proteins was detected by western blotting. Cleavage of caspase-3 and PARP was induced following exposure of CT26 cells to GRWE for 24 h. In addition, GRWE treatment reduced the expression of caspase-8, caspase-9, Bcl-2, and Bcl-xL and increased the protein level of Bax in CT26 cells (Fig. 3C).

GRWE induces apoptosis via AMPK activation in CT26 cells. Activation of AMPK inhibits cell proliferation by promoting apoptosis of cancer cells. Various anticancer drugs and plant extracts can induce AMPK-mediated apoptosis in cancer cells (30). A previous study reported that PGG, a component of Galla Rhois, induced breast cancer cell death through phosphorylation of AMPK (31). Therefore, we hypothesized that apoptosis of CT26 cells by GRWE was related to activation of AMPK. As revealed in Fig. 4A, phosphorylation of AMPK was increased after GRWE treatment in a time-dependent manner. To confirm whether GRWE-induced AMPK phosphorylation was involved in apoptosis of CT26 cells, AMPK inhibitor compound C (20 μM) was pre-treated to CT26 cells for 4 h, and then treated with GRWE (20-100 μg/ml) for 72 h. Blockage of AMPK activation recovered GRWE-decreased viability of CT26 cells (Fig. 4B). To further investigate whether apoptosis-related factors were regulated by AMPK activation, the protein levels of cleaved caspase-3 and PARP were detected in compound C and GRWE-treated CT26 cells. Cleavage of caspase-3 and PARP was induced following treatment with GRWE, whereas AMPK inhibitor compound C suppressed this effect of GRWE (Fig. 4C). Several studies have shown that AMPK activators induce apoptosis via modulation of the MAPK pathway in human cancer cells (32). AMPK activation induces apoptosis via the downregulation of ERK in cancer cells, and AMPK activator AICAR inhibits p38 MAPK (33,34). Based on these studies, we confirmed whether GRWE could regulate the phosphorylation of ERK and p38. As expected, GRWE reduced the phosphorylation of ERK and p38 (Fig. 4D). These results indicated that GRWE-induced apoptosis occurred through the AMPK-ERK/p38 signaling pathway.

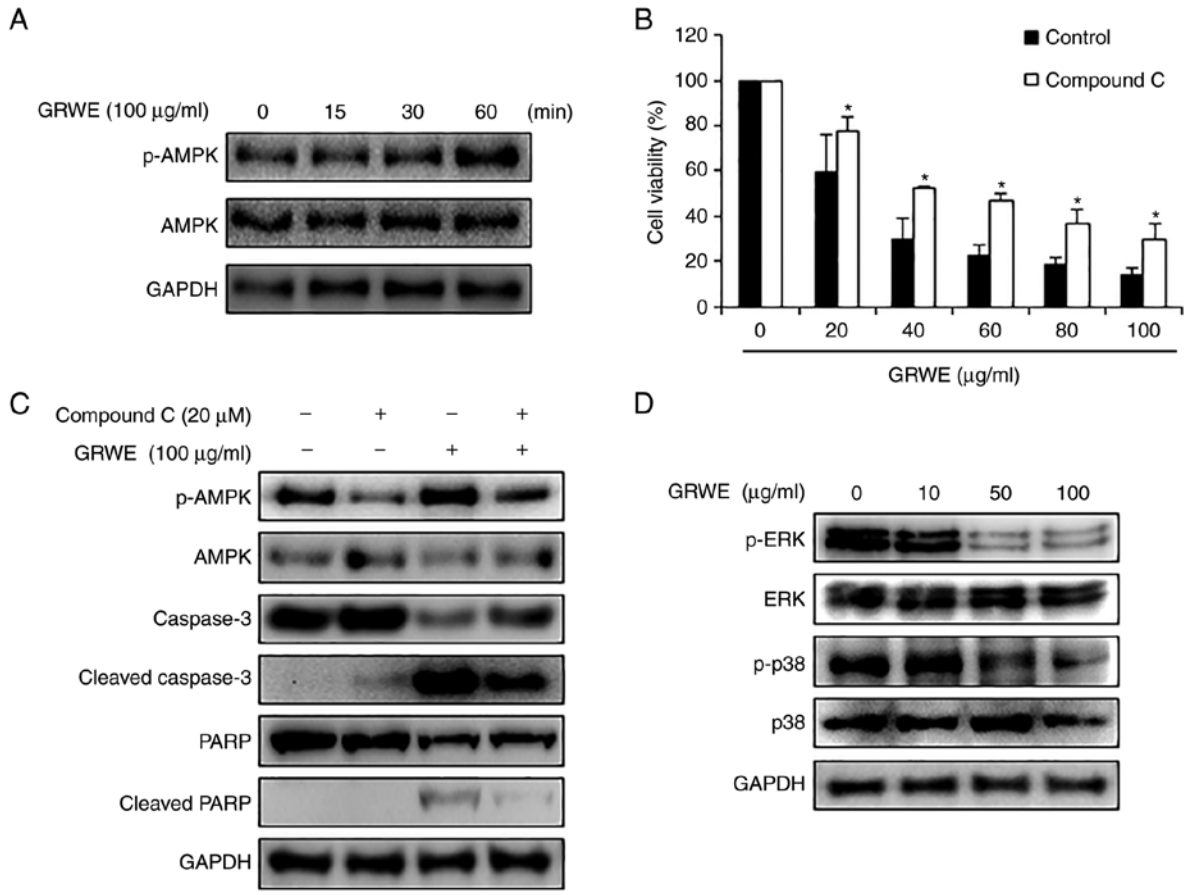

Figure 4. GRWE regulates the expression of apoptotic proteins via the AMPK and ERK/p38 signaling pathways. (A) Phosphorylation of AMPK in GRWE-treated CT26 cells was detected by western blotting. Cells were treated with GRWE (100 μg/ml) for 15, 30, and 60 min. (B) Cell viability of GRWE-treated CT26 cells after pretreatment of compound C (20 μM) for 4 h. Cell viability was measured using WST-8 reagent after 72 h of GRWE treatment. *P<0.05 compared with the control group. (C) After compound C (20 μM) pretreatment for 4 h, CT26 cells were treated with GRWE (100 μg/ml) for 24 h. The expression of p-AMPK, AMPK, caspase-3, cleaved caspase-3 and cleaved PARP was detected by western blotting. (D) Phosphorylation of ERK and p38 in GRWE-treated CT26 cells for 24 h was confirmed by western blotting. GRWE, Galla Rhois water extract; AMPK, adenosine monophosphate-activated protein kinase.

Effect of GRWE on the expression of EMT markers in CT26 cells. Gene expression analysis was conducted to elucidate whether GRWE regulated the expression of EMT markers, which are involved in metastatic properties of cancer cells. The mRNA level of epithelial phenotypic marker E-cadherin was upregulated after GRWE treatment (Fig. 5A). In addition, the expression of mesenchymal phenotypic markers N-cadherin, vimentin, and Twist was downregulated in GRWE-treated CT26 cells (Fig. 5B-D). Consistent with the mRNA expression levels, GRWE increased the protein levels of E-cadherin and reduced N-cadherin, vimentin, and Twist expression (Fig. 5E and F). We confirmed GRWE-mediated enhanced expression of E-cadherin by immunofluorescence (Fig. 5G).

Effect of GRWE on the migratory and invasive abilities of CT26 cells. After EMT, cancer cells acquire migratory and invasive properties, resulting in metastasis (35). We performed a wound healing assay to explore the effect of GRWE on the migration of CT26 cells. Following 48 h of incubation, the control cells were more proficient in repairing wounds as compared with the GRWE-treated cells. Treatment with GRWE (1, 5, and 10 μg/ml) resulted in the inhibition of the migratory ability of CT26 cells (Fig. 6A). An invasion assay was carried out using a Matrigel-coated Transwell chamber to further investigate the effect of GRWE on the invasion ability of CT26 cells. As revealed in Fig. 6B, the infiltration of CT26 cells in the Matrigel-coated membrane was decreased following GRWE treatment in a dose-dependent manner. In addition, we assessed the mRNA expression of matrix metalloproteinase (MMP)-2 and MMP-9 using real-time RT-PCR and determined that MMP-2 and MMP-9 expression was downregulated by GRWE treatment (Fig. 6C). We also analyzed the activity of MMP-2 and MMP-9 by gelatin zymography and found that GRWE reduced the activity of MMP-2 and MMP-9 in CT26 cells (Fig. 6D).

Effect of GRWE on the lung metastatic ability of CT26 cells. To investigate whether GRWE inhibited the lung metastatic ability of CRC cells in mice, we employed an experimental lung metastatic model. Body weight remained unaffected following treatment with GRWE (Fig. 7A). After intravenous injection of CT26 cells, the number of metastatic tumor nodules in the lungs increased initially but were reduced after the oral administration of GRWE (250 and 500 mg/kg) for 2 weeks (Fig. 7B and C).

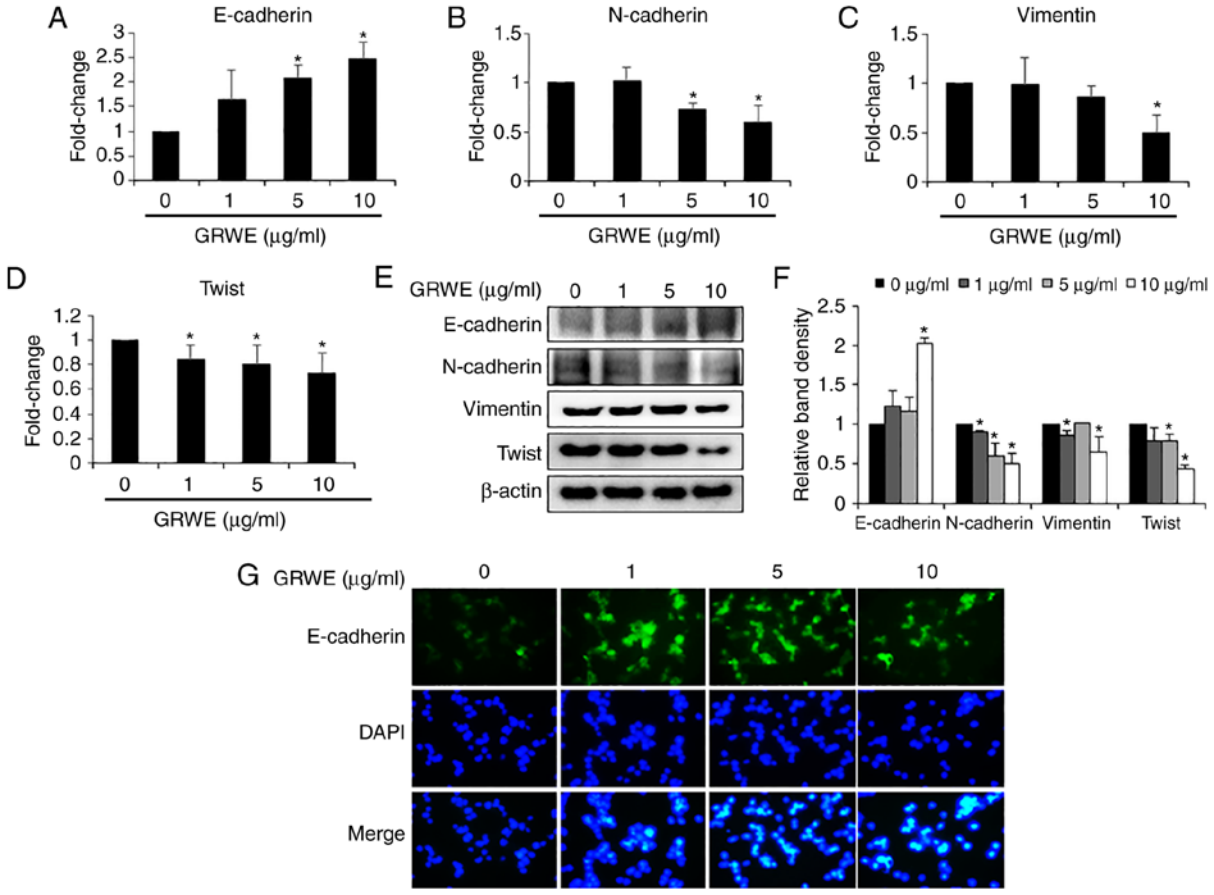

Figure 5. GRWE regulates the expression of EMT markers. CT26 cells were treated for 24 h with GRWE (1, 5, and 10 μg/ml). The mRNA expression levels of EMT markers were measured by real-time RT-PCR. (A) Epithelial marker: E-cadherin. (B-D) Mesenchymal markers: N-cadherin, vimentin, and twist. Results are expressed as the mean ± SD of three independent experiments. *P<0.05. (E) The expression of EMT-related proteins was detected by western blotting. (F) The density of western blot bands was quantified by densitometric analysis using ImageJ software. (G) The expression of E-cadherin was detected by immunofluorescence assay (x200, magnification). GRWE, Galla Rhois water extract; EMT, epithelial-mesenchymal transition.

Discussion

This study elucidated the inhibitory effect of GRWE on colorectal metastasis using metastatic CRC cells and an experimental lung metastatic model. Galla Rhois has been used to treat various diseases in East Asia. Although the pharmacological actions of Galla Rhois are well studied, its effects on cancer as well as the mechanism underlying the anticancer effects remain to be addressed.

Malignant tumors develop from cancer cells that are resistant to programmed cell death and undergo indefinite proliferation. Therefore, induction of apoptosis contributes to the restriction of cancer progression, and many approved cancer therapies induce apoptosis in cancer cells (36,37). According to recent studies, GRWE may induce cell death in various human cancer cell lines, including HCT116, AGS, MDA-MB-231, A549, and SK-Hep-1. In particular, ellagic acid promoted apoptosis of human CRC cell line HCT116 via caspase-dependent pathway (25). In the present study, we observed that GRWE significantly inhibited the proliferation of CRC cell lines CT26 and HT29 (Fig. 2A and B). The antiproliferative effect of GRWE was exerted through the induction of apoptosis in CT26 cells (Fig. 3A and B).

The initiation of apoptosis occurs through strictly controlled mechanisms. Apoptosis is mediated by two basic signaling pathways-the extrinsic and intrinsic pathway. The extrinsic pathway is triggered through the binding of death ligands to receptors. Activated caspase-8 subsequently induces cleavage of caspase-3 and PARP or activates the mitochondria-mediated intrinsic pathway. The intrinsic pathway is activated by several stimuli such as DNA damage and deprivation of cell survival factors (38,39). This is controlled by a series of Bcl-2 family members. The anti-apoptotic proteins Bcl-2 and Bcl-xL arrest the emission of cytochrome *c*, while the pro-apoptotic protein Bax promotes the release of cytochrome *c* from mitochondria. The release of the cytochrome *c* is followed by the activation of downstream caspases (caspase-9 and caspase-3), thereby leading to apoptosis (40). In the present study, GRWE induced the cleavage of caspase-3 and PARP and reduced the expression of caspase-8 and caspase-9. Furthermore, the expression of anti-apoptotic proteins Bcl-2 and Bcl-xL were decreased, whereas the expression of pro-apoptotic protein Bax was increased following GRWE treatment (Fig. 3C). These results demonstrated that GRWE-induced apoptosis was mediated through the extrinsic and intrinsic apoptotic pathways in CT26 cells.

Activation of AMPK can inhibit proliferation of cancer cells by inducing apoptosis (30). In addition, AMPK activators induce apoptosis via the MAPKs signaling pathway in human cancer cells (32). Phosphorylation of ERK generally suppresses

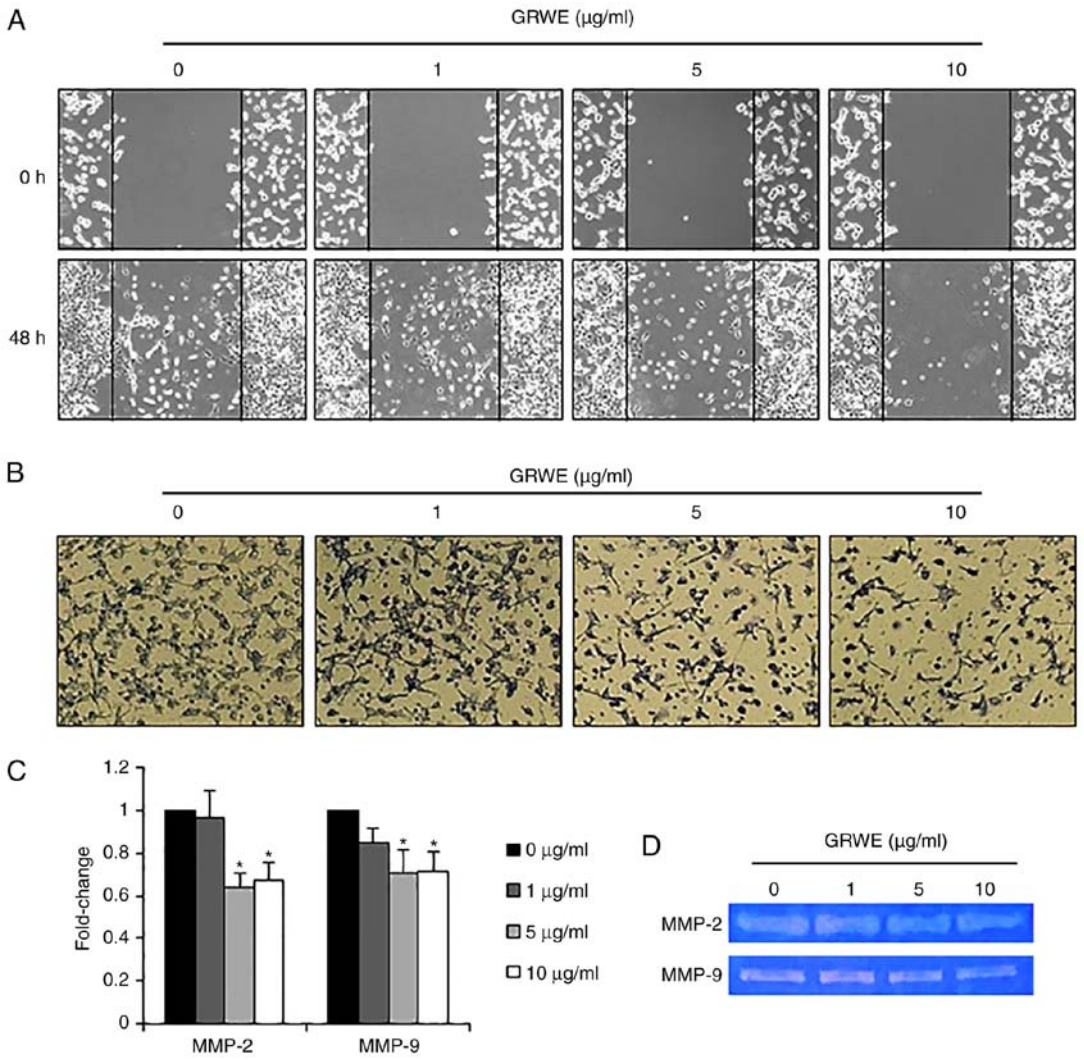

Figure 6. GRWE suppresses migration and invasion abilities of CT26 cells. (A) The migration ability of CT26 cells was determined by wound healing assay following treatment with GRWE at the indicated concentrations. Images were captured after 48 h of incubation. (B) A Matrigel invasion assay was conducted to investigate the invasion ability of CT26 cells following treatment with the indicated concentrations of GRWE. After 24 h of incubation, the inner sides of the chamber were fixed and stained. (C and D) The mRNA expression level and activity of MMPs were measured by (C) real-time RT-PCR and (D) gelatin zymography, respectively. Results are expressed as the mean ± SD of three independent experiments. *P<0.05. GRWE, Galla Rhois water extract.

apoptosis of cells by regulating apoptotic protein expression such as the Bcl-2 family members and caspases (41,42). p38 MAPK can also modulate survival, growth and differentiation of various cancer cells (43-45). Several studies have reported that p38 MAPK inhibited autophagy and apoptosis, thereby promoting survival of CRC cells (34,46). In the present study, GRWE induced the phosphorylation of AMPK and inhibited the phosphorylation of ERK and p38 (Fig. 4A and D). Inhibition of AMPK activity partially recovered cell viability and the expression of apoptosis-related proteins in GRWE-treated CT26 cells (Fig. 4B and C). Based on these results, GRWE induced apoptosis of CRC cells via the AMPK-ERK/p38 signaling pathway.

Epithelial cells are closely connected to surrounding cells by tight junctions, adherens junctions and gap junctions. In addition, these cells display cell polarity and are attached by a basal lamina. Conversely, mesenchymal cells rarely form cell-cell junctions, interplay only focally, and lack polarity. During EMT, the stationary cancer cells gain motility and invasiveness. Therefore, the EMT process plays an important role in promoting metastasis. EMT is induced by the interaction of extracellular signals. The activation of the signaling pathway enhances transcriptional regulators, including Snail, Slug, and Twist. The main target of transcriptional regulators is the suppression of E-cadherin, the cell-cell adhesion molecule (47,48). The downregulation of E-cadherin is often accompanied by the upregulation of N-cadherin, the invasion promoter molecule (49). In the present study, GRWE at non-cytotoxic concentrations increased the expression of the epithelial marker E-cadherin and reduced the expression of mesenchymal markers, including N-cadherin, vimentin, and twist (Fig. 5). These results indicated that GRWE may suppress colorectal metastasis through the inhibition of the EMT process.

MMPs play a critical role in many events during malignant transformation, including tumor growth, angiogenesis, invasion, and metastasis. EMT of cancer cells contributes to the production of MMPs, and increased MMPs promote the pathogenic EMT process (35). In particular, MMP-2 and MMP-9 may induce degradation of ECM, thereby facilitating

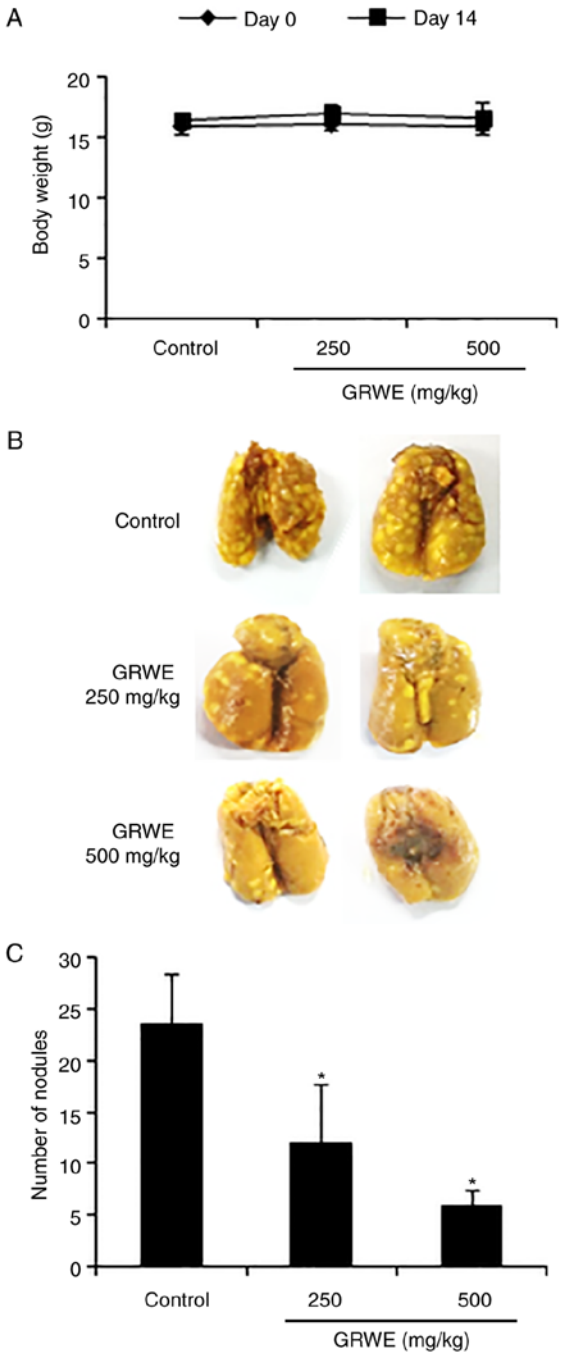

Figure 7. GRWE inhibits colorectal lung metastasis. Mice were divided into three groups (n=8) and GRWE (250 or 500 mg/kg) was administered. (A) The body weights of mice were measured. (B) Lungs were resected and stained with Bouin's solution for the evaluation of tumor formation. (C) The number of tumor nodules was counted. Results are expressed as the mean ± SD of three independent experiments. *P<0.05. GRWE, Galla Rhois water extract.

migration and invasion in most cancers (50). The non-cytotoxic concentrations of GRWE inhibited the motility and invasiveness of CT26 cells (Fig. 6A and B). Moreover, the expression and activity of MMP-2 and MMP-9 were suppressed by GRWE treatment (Fig. 6C and D). These results confirmed that GRWE may inhibit the migration and invasion ability through the reduction in MMP-2 and MMP-9 expression.

In the present study, HPLC chromatogram of GRWE revealed characteristic peaks for GT (25.1, 25.5, 26.7, 27.0 and 27.3 min) (Fig. 1), indicative of the presence of GT in GRWE. The GT-rich *Caesalpinia spinosa* fraction is known to exert antitumor and anti-metastatic effects in murine breast cancer models through the reduction of serum interleukin (IL)-6 level and cell cycle arrest in the S phase (51,52). Moreover, GT inhibited primary CRC tumors by suppressing the expression of nuclear factor-κB (NF-κB)-regulated inflammatory cytokines and proliferation of HT29 and HCT116 cells (53). GT present in GRWE was expected to exert an anti-metastatic effect on CRC cells. Further studies are required to evaluate the potential of GT and other GRWE contents to inhibit metastatic abilities of CRC cells and colorectal metastasis in *in vivo* models.

To the best of our knowledge, this is the first study to demonstrate the anti-metastatic potential of GRWE against metastatic CRC cells *in vitro* and *in vivo*. In summary, GRWE decreased the lung metastasis of CRC cells by inducing apoptosis and suppressing metastatic phenotypes, including EMT, migration, and invasion. Thus, GRWE may be used as a potential therapeutic agent for the treatment of colorectal metastasis.

Acknowledgements

Not applicable.

Funding

The present study was supported by the Wonkwang University in 2016.

Availability of data and materials

The datasets used during the present study are available from the corresponding author upon reasonable request.

Authors' contributions

JYK and SHH designed the experiments. JGM and JYK wrote the manuscript. JGM, JYK, YHH, SHP and HDJ carried out the experiments. SL performed the HPLC analysis. SHH supervised the entire experiments and analyses. All authors read and approved the manuscript and agree to be accountable for all aspects of the research in ensuring that the accuracy or integrity of any part of the work are appropriately investigated and resolved.

Ethics approval and consent to participate

The *in vivo* experiment was approved and performed in accordance with the internationally accepted principles for the care and use of laboratory animals by the Institutional Animal Care and Use Committee of Wonkwang University (WKU16-11).

Patient consent for publication

Not applicable.

Competing interests

The authors declare that they have no competing interests.

References

1. Haggar FA and Boushey RP: Colorectal cancer epidemiology: Incidence, mortality survival, and risk factors. Clin Colon Rectal Surg 22: 191-197, 2009.
2. Torre LA, Bray F, Siegel RL, Ferlay J, Lortet-Tieulent J and Jemal A: Global cancer statistics, 2012. CA Cancer J Clin 65: 87-108, 2015.
3. Dromain C, Caramella C, Dartigues P, Goere D, Ducreux M and Deschamps F: Liver, lung and peritoneal metastases in colorectal cancers: Is the patient still curable? What should the radiologist know. Diagn Interv Imaging 95: 513-523, 2014.
4. Tsoulfas G, Pramateftakis MG and Kanellos I: Surgical treatment of hepatic metastases from colorectal cancer. World J Gastrointest Oncol 3: 1-9, 2011.
5. Dahabre J, Vasilaki M, Stathopoulos GP, Kondaxis A, Iliadis K, Papadopoulos G, Stathopoulos J, Rigatos S, Vasilikos K and Koutantos J: Surgical management in lung metastases from colorectal cancer. Anticancer Res 27: 4387-4390, 2007.
6. Kim HJ, Kye BH, Lee JI, Lee SC, Lee YS, Lee IK, Kang WK, Cho HM, Moon SW and Oh ST: Surgical resection for lung metastases from colorectal cancer. J Korean Soc Coloproctol 26: 354-358, 2010.
7. Martin TA, Ye L, Sanders AJ, Lane J and Jiang WG: Cancer invasion and metastasis: Molecular and cellular perspective. In: Metastatic Cancer: Clinical and Biological Perspectives. Jandial R (ed). Landes Bioscience, Austin, pp135-168, 2013.
8. Mishra J, Drummond J, Quazi SH, Karanki SS, Shaw JJ, Chen B and Kumar N: Prospective of colon cancer treatments and scope for combinatorial approach to enhanced cancer cell apoptosis. Crit Rev Oncol Hematol 86: 232-250, 2013.
9. Kalluri R and Weinberg RA: The basics of epithelial-mesenchymal transition. J Clin Inv est 119: 1420-1428, 2009.
10. Garg M: Epithelial-mesenchymal transition-activating transcription factors-multifunctional regulators in cancer. World J Stem Cells 5: 188-195, 2013.
11. Heerboth S, Housman G, Leary M, Longacre M, Byler S, Lapinska K, Willbanks A and Sarkar S: EMT and tumor metastasis. Clin Transl Med 4: 6, 2015.
12. Lowe SW and Lin AW: Apoptosis in cancer. Carcinogenesis 23: 485-495, 2000.
13. Olsson M and Zhivotovsky B: Caspases and cancer. Cell Death Differ 18: 1441-1449, 2011.
14. Herceg Z and Wang ZQ: Functions of poly(ADP-ribose) polymerase (PARP) in DNA repair, genomic integrity and cell death. Mutat Res 477: 97-110, 2001.
15. Tsujimoto Y: Role of Bcl-2 family proteins in apoptosis: Apoptosomes or mitochondria? Genes Cells 3: 697-707, 1998.
16. Wong RS: Apoptosis in cancer: From pathogenesis to treatment. J Exp Clin Cancer Res 30: 87, 2011.
17. Monteverde T, Muthalagu N, Port J and Murphy DJ: Evidence of cancer-promoting roles for AMPK and related kinases. FEBS J 282: 4658-4671, 2015.
18. Schultze SM, Hemmings BA, Niessen M and Tschopp O: PI3K/AKT, MAPK and AMPK signalling: Protein kinases in glucose homeostasis. Expert Rev Mol Med 14: e1, 2012.
19. Hardie DG, Ross FA and Hawley SA: AMPK: A nutrient and energy sensor that maintains energy homeostasis. Nat Rev Mol Cell Biol 13: 251-262, 2012.
20. Rehman G, Shehzad A, Khan AL and Hamayun M: Role of AMP-activated protein kinase in cancer therapy. Arch Pharm 347: 457-468, 2014.
21. Baba Y, Nosho K, Shima K, Meyerhardt JA, Chan AT, Engelman JA, Cantley LC, Loda M, Giovannucci E, Fuchs CS and Ogino S: Prognostic significance of AMP-activated protein kinase expression and modifying effect of MAPK3/1 in colorectal cancer. Br J Cancer 103: 1025-1033, 2010.
22. Ahn YJ, Lee CO, Kweon JH, Ahn JW and Park JH: Growth-inhibitory effects of Galla Rhois-derived tannins on intestinal bacteria. J Appl Microbiol 84: 439-443, 1998.
23. Go J, Kim JE, Koh EK, Song SH, Seong JE, Park CK, Lee HA, Kim HS, Lee JH, An BS, *et al*: Hepatotoxicity and nephrotoxicity of gallotannin-enriched extract isolated from Galla Rhois in ICR mice. Lab Anim Res 31: 101-110, 2015.
24. Kim SH, Park HH, Lee S, Jun CD, Choi BJ, Kim SY, Kim SH, Kim DK, Park JS, Chae BS, *et al*: The anti-anaphylactic effect of the gall of *Rhus javanica* is mediated through inhibition of histamine release and inflammatory cytokine secretion. Int Immunopharmacol 5: 1820-1829, 2005.
25. Yim NH, Gu MJ, Hwang YH, Cho WK and Ma JY: Water extract of Galla Rhois with steaming process enhances apoptotic cell death in human colon cancer cells. Integr Med Res 5: 284-292, 2016.
26. Lee HJ, Seo NJ, Jeong SJ, Park Y, Jung DB, Koh W, Lee HJ, Lee EO, Ahn KS, Ahn KS, *et al*: Oral administration of penta-O-galloyl-β-D-glucose suppresses triple-negative breast cancer xenograft growth and metastasis in strong association with JAK1-STAT3 inhibition. Carcinogenesis 32: 804-811, 2011.
27. Deiab S, Mazzio E, Eyunni S, McTier O, Mateeva N, Elshami F and Soliman KF: 1,2,3,4,6-Penta-*O*-galloylglucose within Galla Chinensis inhibits human LDH-A and attenuates cell proliferation in MDA-MB-231 breast cancer cells. Evid Based Complement Alternat Med 2015: 276946, 2015.
28. Ata N, Oku T, Hattori M, Fujii H, Nakajima M and Saiki I: Inhibition by galloylglucose (GG6-10) of tumor invasion through extracellular matrix and gelatinase-mediated degradation of type IV collagens by metastatic tumor cells. Oncol Res 8: 503-511, 1996.
29. Livak KJ and Schmittgen TD: Analysis of relative gene expression data using real-time quantitative PCR and the $2^{-\Delta\Delta C_T}$ method. Methods 25: 402-408, 2001.
30. Chen MB, Zhang Y, Wei MX, Shen W, Wu XY, Yao C and Lu PH: Activation of AMP-activated protein kinase (AMPK) mediates plumbagin-induced apoptosis and growth inhibition in cultured human colon cancer cells. Cell Signal 25: 1993-2002, 2013.
31. Chai Y, Lee HJ, Shaik AA, Nkhata K, Xing C, Zhang J, Jeong SJ, Kim SH and Lu J: Penta-O-galloyl-beta-D-glucose induces G_1 arrest and DNA replicative S-phase arrest independently of cyclin-dependent kinase inhibitor 1A, cyclin-dependent kinase inhibitor 1B and P53 in human breast cancer cells and is orally active against triple negative xenograft growth. Breast Cancer Res 12: R67, 2010.
32. Li W, Saud SM, Young MR, Chen G and Hua B: Targeting AMPK for cancer prevention and treatment. Oncotarget 6: 7365-7378, 2015.
33. Plews RL, Mohd Yusof A, Wang C, Saji M, Zhang X, Chen CS, Ringel MD and Phay JE: A novel dual AMPK activator/mTOR inhibitor inhibits thyroid cancer cell growth. J Clin Endocrinol Metab 100: E748-E756, 2015.
34. Kim MJ, Yun H, Kim DH, Kang I, Choe W, Kim SS and Ha J: AMP-activated protein kinase determines apoptotic sensitivity of cancer cells to ginsenoside-Rh2. J Ginseng Res 38: 16-21, 2014.
35. Son H and Moon A: Epithelial-mesenchymal transition and cell invasion. Toxicol Res 26: 245-252, 2010.
36. Plati J, Bucur O and Khosravi-Far R: Apoptotic cell signaling in cancer progression and therapy. Integr Biol 3: 279-296, 2011.
37. Takeda K, Stagg J, Yagita H, Okumura K and Smyth MJ: Targeting death-inducing receptors in cancer therapy. Oncogene 26: 3745-3757, 2007.
38. Su Z, Yang Z, Xu Y, Chen Y and Yu Q: Apoptosis, autophagy, necroptosis, and cancer metastasis. Mol Cancer 14: 48, 2015.
39. Hideshima T and Anderson KC: Molecular mechanisms of novel therapeutic approaches for multiple myeloma. Nat Rev Cancer 2: 927-937, 2002.
40. Han YH, Kee JY, Kim DS, Mun JG, Jeong MY, Park SH, Choi BM, Park SJ, Kim HJ, Um JY, *et al*: Arctigenin inhibits lung metastasis of colorectal cancer by regulating cell viability and metastatic phenotypes. Molecules 21: E1135, 2016.
41. Huang T, Xiao Y, Yi L, Li L, Wang M, Tian C, Ma H, He K, Wang Y, Han B, *et al*: Coptisine from rhizoma coptidis suppresses hct-116 cells-related tumor growth in vitro and in vivo. Sci Rep 7: 38524, 2017.
42. Lu Z and Xu S: ERK1/2 MAP kinases in cell survival and apoptosis. IUBMB Life 58: 621-631, 2006.
43. Grossi V, Peserico A, Tezil T and Simone C: p38α MAPK pathway: A key factor in colorectal cancer therapy and chemoresistance. World J Gastroenterol 20: 9744-9758, 2014.
44. Sui X, Kong N, Ye L, Han W, Zhou J, Zhang Q, He C and Pan H: p38 and JNK MAPK pathways control the balance of apoptosis and autophagy in response to chemotherapeutic agents. Cancer Lett 344: 174-179, 2014.
45. Chen L, Mayer JA, Krisko TI, Speers CW, Wang T, Hilsenbeck SG and Brown PH: Inhibition of the p38 kinase suppresses the proliferation of human ER-negative breast cancer cells. Cancer Res 69: 8853-8861, 2009.
46. Thornton TM and Rincon M: Non-classical p38 map kinase functions: Cell cycle checkpoints and survival. Int J Biol Sci 5: 44-51, 2009.

47. Thiery JP and Sleeman JP: Complex networks orchestrate epithelial-mesenchymal transitions. Nat Rev Mol Cell Biol 7: 131-142, 2006.
48. Lindsey S and Langhans SA: Crosstalk of oncogenic signaling pathways during epithelial-mesenchymal transition. Front Oncol 4: 358, 2014.
49. Derycke LD and Bracke ME: N-cadherin in the spotlight of cell-cell adhesion, differentiation, embryogenesis, invasion and signalling. Int J Dev Biol 48: 463-476, 2004.
50. Gialeli C, Theocharis AD and Karamanos NK: Roles of matrix metalloproteinases in cancer progression and their pharmacological targeting. FEBS J 278: 16-27, 2011.
51. Urueña C, Mancipe J, Hernandez J, Castañeda D, Pombo L, Gomez A, Asea A and Fiorentino S: Gallotannin-rich *Caesalpinia spinosa* fraction decreases the primary tumor and factors associated with poor prognosis in a murine breast cancer model. BMC Complement. Altern Med 13: 74, 2013.
52. Zhao T, Sun Q, del Rincon SV, Lovato A, Marques M and Witcher M: Gallotannin imposes S phase arrest in breast cancer cells and suppresses the growth of triple-negative tumors in vivo. PLoS One 9: e92853, 2014.
53. Al-Halabi R, Bou Chedid M, Abou Merhi R, El-Hajj H, Zahr H, Schneider-Stock R, Bazarbachi A and Gali-Muhtasib H: Gallotannin inhibits NFκB signaling and growth of human colon cancer xenografts. Cancer Biol Ther 12: 59-68, 2011.